Review

Cation exchange dynamics confined in a synthetic clay mineral

G. Grassi[1,2,a], L. Michels[2], Z. Rozynek[2,3], M.A.S. Altoé[1], E.C dos Santos[2], C.L.S. da Fonseca[1], R. Droppa Jr.[4], A. Gholamipour-Shirazi[5,6], J.O. Fossum[2,b], and G.J. da Silva[1]

[1] Instituto de Física, Universidade de Brasília, 70.919-970 Brasília – DF, Brazil
[2] Department of Physics, Norwegian University of Science and Technology, 7491 Trondheim, Norway
[3] Institute of Physical Chemistry, Polish Academy of Sciences, Kasprzaka 44/52, 01-224 Warsaw, Poland
[4] Universidade Federal do ABC, 09.210-580 Santo André – SP, Brazil
[5] Laboratório de Microhidrodinâmica e Escoamento em Meios Porosos, Department of Mechanical Engineering, Pontifícia Universidade Católica do Rio de Janeiro, 22.451-263 Rio de Janeiro – RJ, Brazil
[6] Centro de Componentes Semicondutores, Universidade Estadual de Campinas, 13.083-870 Campinas – SP, Brazil

Abstract. In this work we report X-Ray Diffraction (XRD) and Energy Dispersive X-Ray Spectroscopy (EDS) measurements to investigate the confined cation exchange process in saline aqueous suspensions of a synthetic clay mineral from Lithium-Fluorohectorite to Nickel-Fluorohectorite, as well as the reverse process from Nickel-Fluorohectorite to Lithium-Fluorohectorite and also from Lithium-Fluorohectorite to Sodium-Fluorohectorite. The dynamics of these cation exchanges was followed and it was observed that these processes can be faster than 1 minute. The results are compared to the observations on samples prepared by cation exchange procedures for which the exchange process was performed on the time-scale of months.

1 Introduction

The use of clays is broad, essentially because they are abundant and inexpensive [1]. Like other materials such as colloidal systems, polymers, liquid crystals, biomaterials, etc., clays are important materials in advanced materials science [2,3]. Clay minerals have attracted significant attention by scientists from a wide spectrum of disciplines [4]. Since natural clay minerals may have impurities that can 'hide' some of their

[a] e-mail: grassi@unb.br
[b] e-mail: jon.fossum@ntnu.no
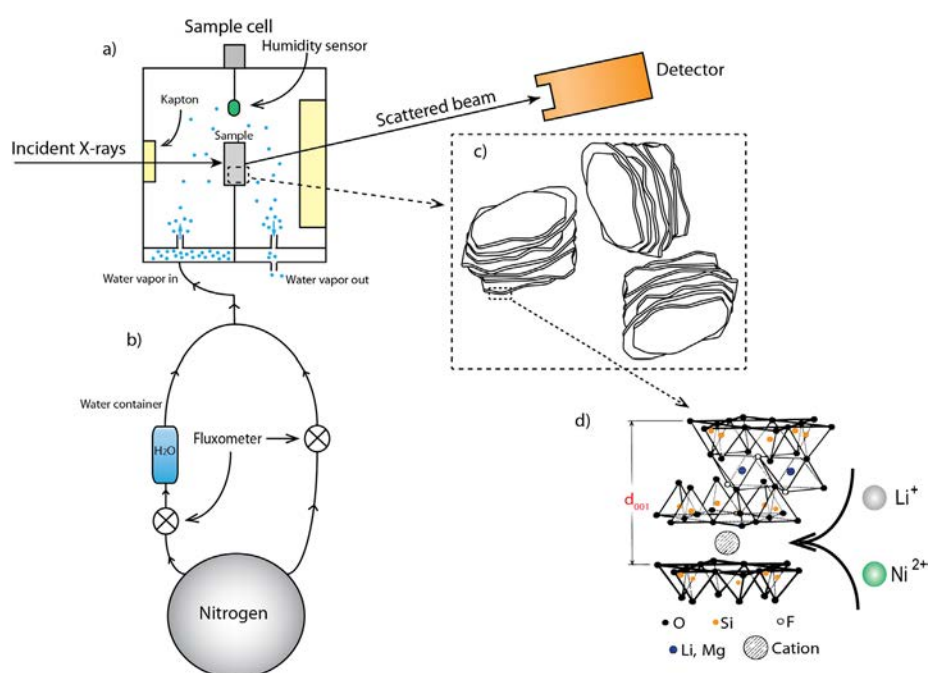
Fig. 1. a) Experimental setup consists of a sample chamber with X-ray windows including RH and temperature sensors. b) RH is controlled by mixing dry and humid flows. c) Fluorohectorite clay mineral particle lamellar stacks. d) The representation of the clay mineral crystallographic structure, indicating the d-spacing given by XRD Bragg peaks.

inherent physical and chemical features, many experiments are performed using synthetic clay minerals, and moreover, synthetic clay minerals are widely used as model systems [5,6].

Clay minerals or nanosilicates are composed of micro-crystalline particles of a small group of minerals. Smectite, which is a group of clay minerals, has a stacking structure, as seen in Fig. 1c. This structure is due to the layered charge properties and the presence of charge compensating interlayer cations between each layer (Fig. 1d). The interlayer ion can be replaced by another ion through ion exchange process[7–14]. These ions serve as face-face or face-edge spacers connected to the clay mineral lamellae, enabling design of porous structures that can be used industrially as molecular selectors [15].

One of the most important properties of smectite is their cation exchange capacity (CEC) [1]. The exchange between cations balancing the negative layer charge and those in solution is reversible and, in general, there is selectivity of one cation over another [16]. Cation exchange of smectite is usually carried out by mixing the clay mineral with an appropriate salt solution of ∼0.5–1 M for 24 h. The clay mineral can then be centrifuged and re-suspended repetitively to remove excess exchangeable cation [1].

Comans [17] showed, by means of gamma-counter experiments on illite clay minerals, that the adsorption, desorption and isotopic exchange of cadmium are slow processes, continuing after weeks of equilibration and it was demonstrated that adsorption approaches equilibrium faster than desorption. The ^{109}Cd percentages for adsorption show only very small differences after 9 and 54 days respectively, whereas the values of desorption, after an initial rapid increase, continue to increase slightly

with time. Isotopic exchange equilibration shows some slight fluctuation, and it seems that it is similar to the adsorption pattern.

The geochemical interest of nuclear power stations and atomic bomb testing in aquatic systems has initiated studies related to ^{65}Zn. Through atomic absorption spectrophotometry, it was demonstrated that during equilibration on illite clay mineral, 100% of isotopic exchangeability of ^{65}Zn with stable absorbed zinc, was achieved within 1 h [18]. Cation exchange of Zn^{2+} was measured using ^{65}Zn as tracer in three different clay minerals: illite, montmorillonite and kaolinite. It was shown that isotopic equilibrium between ^{109}Cd and ^{65}Zn and stable Cd and Zn respectively in two soils was not obtained in 16 h and possibly not even in 72 h [19].

It is interesting to compare clay minerals to other systems. It has been observed that silver cations in solution can quickly and reversibly replace cations of cadmium in nanocrystals of cadmium selenide, resulting in nanocrystals of silver selenide. This cation exchange was observed from X-ray absorption spectroscopy (XAS) experiments in a time-scale of 100 ms [20].

Clay minerals also have the ability to intercalate molecules, such as CO_2 [21] and drug molecules [22]. One of the most studied cases, that yet has not been throughly understood, is the intercalation of water. Several experimental techniques have been used to investigate water dynamics in clay minerals, for example nuclear magnetic resonance spectroscopy [23,24], infrared spectroscopy [25], XAS [15,26–28], or inelastic neutron scattering [39]. Many simulations have been done in order to describe this intercalation process [29].

In the present work, we have used the synthetic smectite fluorohectorite, which has per half unit cell the following chemical formula: $M_x - (Mg_{3-x}Li_x)Si_4O_{10}F_2$ where M is the interlayer cation, Li^+, Na^+ or Ni^{2+} in the present case. Fluorohectorite clay mineral is a 2:1 phyllosilicate, i.e. its crystal planes are composed of two tetrahedral layers, where there is a silicon atom in the center of each site, sandwiching one octahedral monolayer, and with Li or Mg atoms in the center. It is classified as a trioctahedral smectite since Li^+ substitutes for Mg^{2+} in the octahedral sheet sites, which are fully occupied [1]. In the case of this substitution, the x ratio of Li is responsible for the surface net charge of the layers, which form stacks mediated by interlayer cations. In general, the hectorites have OH groups in the apex of the tetrahedral structure, whereas fluorohectorites are different by substitution of Fluorine in each of these apex groups. Particles of fluorohectorite are polydisperse with lateral dimension sizes ranging from the nanometer up to 10 μm [25].

The pH may also play a role for adsorption of guest molecules by clay minerals. As an example, in drug molecules capture and release by clay minerals is significantly affected by pH changes. Studies of ciprofloxacin (CIP) sorption by Na-, Ca- and Al-montmorillonite, suggested that a cation exchange process that depends on the pH of the solution gives rise to drug molecule capture. But for pH values less than 8.7, the amount of the absorbed CIP slightly increases with increasing pH, and for values higher than 8.7, the CIP sorption decreases significantly [29]. In this case, at short time, the dependency to pH is mainly attributed to the modification of CIP, although it is unclear if pH effects on the clay mineral particles themselves play any role [30].

Moreover, here we have studied the dynamics of Ni-fluorohectorite (Ni-Fh) cation exchange process starting from Li-fluorohectorite (Li-Fh) at different pH values. The treatment in acid solution is a common clay mineral chemical modification (activated clay minerals) [1]. The duration of such treatment is typically several hours [31,32], and it may cause the water molecules to access the interlayer spaces more easily [33] thus facilitating the cation exchange process [34]. In addition we have also used Energy Dispersive Spectroscopy (EDS) to observe cation exchange transition from Li-Fh to Na-Fh, which we compare and discuss in the context of the Ni-Fh - Li-Fh exchange.

Table 1. Summary of samples preparations.

Sample	$NiCl_2, 6H_2O$ weight (g)	Li-Fh (g)	Aqueous HCl Volume (mL)	pH at 23 °C
1	0.3531	1.0015	200	2.02
2	0.3538	1.0051	200	7.01

2 Methods

2.1 Sample preparation

2.1.1 Cation Exchange from Li-Fh to Ni-Fh

Two groups of Ni-Fh samples were prepared from a cation exchange procedure starting from Li-Fh.

The first group of samples was prepared by a "traditional" cation exchange method that takes advantage of a dialysis column, in which the powder is collected during typically , several months [34–39].

The second group of Ni-Fh samples involve Ni-Fh samples prepared through a multi-step cation exchange process comprising of dissolving Li-Fh clay mineral, adjusting pH by hydrochloric acid and sampling at different time intervals,. According to the stoichiometric calculations the required amounts of the $NiCl_26(H_2O)$ salt to exchange the Li interlayer cations were estimated, (Table 1) and added to the initial Li-Fh clay mineral solution. The samples were prepared at, pH = 2 and pH = 7 respectively.

For pH = 2, samples were taken at time intervals of 1, 20, 40 and 60 minutes and for pH = 7 at time intervals of 1, 5, 30 and 60 minutes.

For preparing each sample 2 mL of suspension was taken and dried quickly using a vacuum filtration system in order to interrupt the cation exchange process. The solid material powder left behind on the filter paper (Magna nylon membrane filter, 0.45 um, Osmonics) after filtration was then used for XRD measurements (XRD2 beamline at LNLS, Campinas, Brazil).

#### 2.1.2 Cation exchange from Ni-Fh to Li-Fh

To investigate the process reversibility we performed a cation exchange starting from Ni-Fh (prepared by the above mentioned procedure) to Li-Fh. This sample was prepared dissolving 1 g of Ni-Fh and 0.62 g of LiCl salt in 200 ml of water solution at pH = 2. The sample was extracted after 5 minutes and processed through the above mentioned steps.

2.2 Experimental setup

2.2.1 XRD setup

To compare the samples at the same relative humidity (RH) condition a cell was specially designed in order to keep the RH stable at 27.40%, which is the room RH value. To create a stable RH medium we used a mixture of dry (N_2) and humid air ($N_2 + H_2O$), while keeping the sample at fixed temperature of 25 ºC using a thermal bath, as shown in Fig. 1.
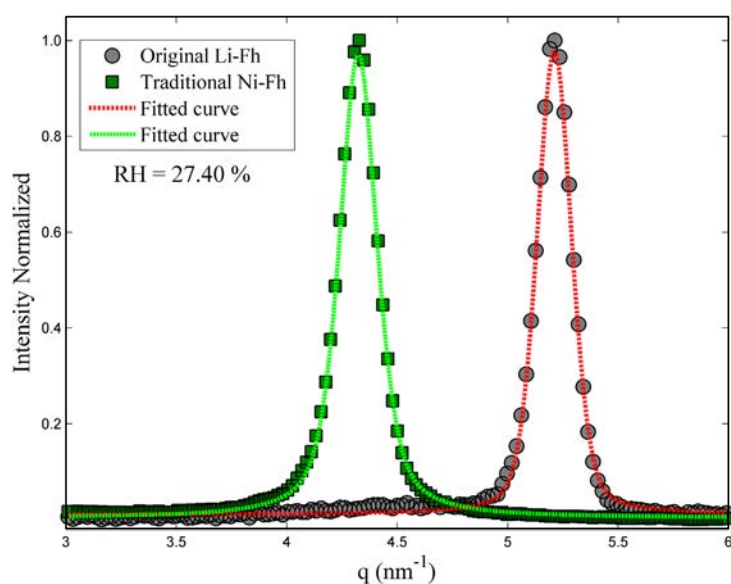
Fig. 2. (001) Bragg peaks of original Li-Fh and traditional Ni-Fh, both at 27.40% of RH, with their respective peak positions q_c. Both curves were fitted with the pseudo-Voigt model.

XRD measurements were conducted near the (001) clay mineral stacking Bragg peak for each sample and the data were compared with those of "traditional" Ni-Fh and the "original" Li-Fh (i.e. which is the starting point for all the samples studied here) always at the same RH and temperature environment. The "original" Li-Fh and "traditional" Ni-Fh were studied utilizing a Small Angle XRay Scattering (SAXS) system NanoSTAR, (Bruker AXS), while the cation exchanged samples were investigated by XRD (XRD2 beamline, Brazilian Synchrotron Light Laboratory (LNLS)).

2.2.2 EDS setup

The energy dispersive spectroscopy (EDS) experiment, which gives information about the sample's elemental composition, was performed using Scanning Electron Microscope Hitachi S-3400N, and it was used to observe cation exchange transition, from the "original" Li-Fh to Na-Fh. Also in the EDS experiments, the powder sample was extracted from a water solution of Li-Fh and NaCl salt after 5 minutes of mixing.
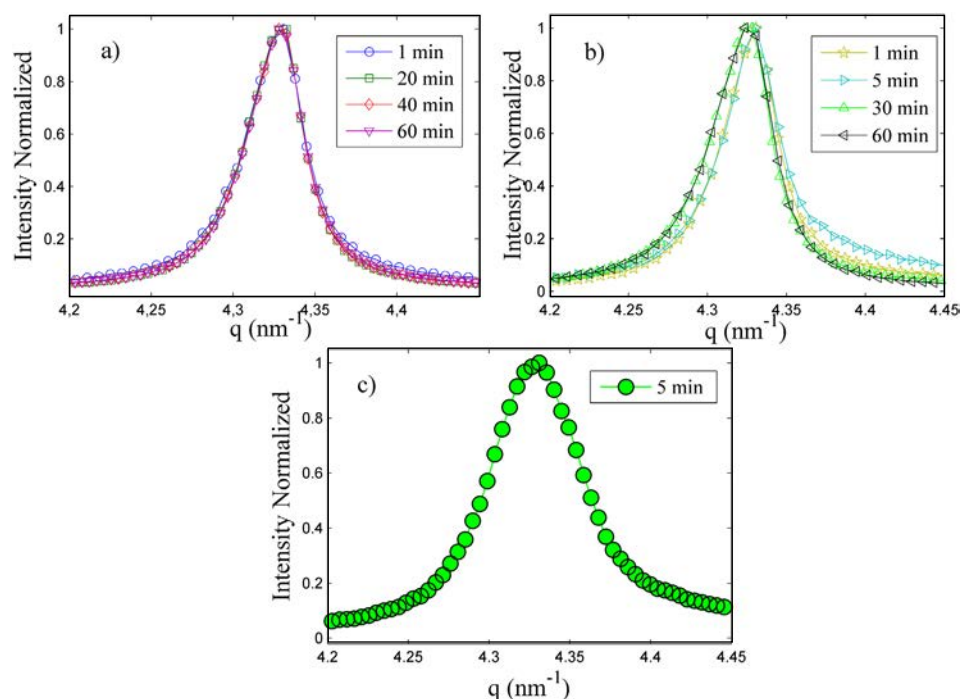
3 Results

3.1 XRD

The experimental Bragg (001) peak intensity, normalized to the maximum intensity, as a function of scattering vector, q, obtained from the original Li-Fh and traditional Ni-Fh at $RH = 27.40\%$ are shown in Fig. 2.

The peak positions were obtained by fitting pseudo-Voigt profiles (Eq. (1)).

$$\Phi(q) = \frac{2\eta}{\pi\Gamma(1 + 4(q - q_c)^2)} + 2\frac{1 - \eta}{\Gamma}\left(\frac{\ln 2}{\pi}\right)^{1/2} e^{-4\ln 2(q - q_c)^2/\Gamma^2} \qquad (1)$$

Fig. 3. Powder samples extracted of a water solution of original Li-Fh and NiCl$_2$.6(H$_2$O) collected at different times after initial preparation for: a) pH = 2 and b) pH = 7. c) Powder sample extracted of a water solution of traditional Ni-Fh and LiCl collected 5 minutes after initial preparation at pH = 2.

where Γ is the experimental width at the half maximum of the curves and η is a mixing constant that ranges from zero to one, and is responsible for changing the shape of the resulting curve from Gaussian to Lorentzian. $\tilde{A}$ and η are related to the widths of the Gaussian, Γ_G, and Lorentzian Γ_L, components by a well-known power law [15]. The linewidth of the Gaussian component is generally attributed to the instrumental resolution and the Lorentzian contribution is related to the size or thickness of crystallized domains.

Figure 2 shows the Bragg scattering peak positions for two reference samples, the original Li-Fh and traditional Ni-Fh. The Li-Fh has peak position at:

$$q_c = (5.211 \pm 0.001) \ \text{nm}^{-1},$$

while Ni-Fh has its peak position at:

$$q_c = (4.324 \pm 0.001) \ \text{nm}^{-1},$$

both at the same condition of temperature and $RH = 27.40\%$.

The peaks presented in Fig. 2 were recorded to be used as references for the (*001*) peaks of the powder extracted from the water solution of Li-Fh and NiCl$_2$.6(H$_2$O) salt at the same temperature and RH conditions. The Bragg peak position identifies which cation is inside the interlayer space. The peaks obtained from the extracted powder samples are shown in Fig. 3.

Figure 3 shows the (*001*) peaks of the powder samples extracted of a water solution of Li-Fh and NiCl$_2$.6(H$_2$O) collected at different times after initial preparation for (a) pH = 7 and (b) pH = 2 respectively. Figure 3c shows the result of the cation
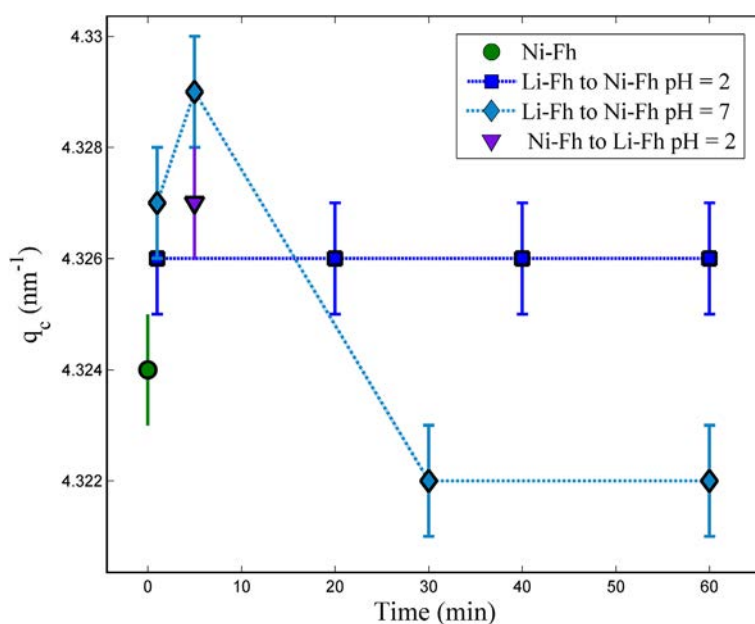
Fig. 4. Peak positions of the traditional Ni-Fh, the samples extracted from the water solution of Li-Fh with $NiCl_26(H_2O)$ as function of time for pH = 2 and pH = 7 and the sample extracted from the water solution of traditional Ni-Fh with LiCl. One can note that the peak position of the original Li-Fh is 5.211 which does not appear at this scale.

exchange from the traditional Ni-Fh to Li-Fh and it shows the (*001*) peak of the powder extracted from a water solution of Ni-Fh with LiCl salt at pH = 2 collected after 5 minutes.

In order to obtain the values of the peak positions as function of time, it was used Eq. (1) and results are show in Fig. 4.

Figure 4 shows that the peak positions from the samples obtained from the $NiCl_26(H_2O)$ salt water solution of original Li-Fh and the LiCl salt water solution of traditional Ni-Fh does not change considerably. Also the pH does not have an observable influence on the peak position. The peak positions for both original Li-Fh to Ni-Fh and from the traditional Ni-Fh to Li-Fh have the same order of magnitude. The mean value of the peak positions for the former is $q_c = (4.326 \pm 0.002) \, nm^{-1}$ and the peak position of the latter is $q_c = (4.327 \pm 0.001) \, nm^{-1}$.

All the XRD measurements were done under the same conditions of temperature and RH as described above.

3.2 EDS

An EDS spectrum shows the chemical composition of the sample. The powder collected after 5 minutes of mixture of Li-Fh and NaCl in water was measured. Figure 5 shows the measured intensity (counts/eV) as a function of the energy for 3 different samples.

In the left panel of Fig. 5a EDS spectrum of pure Li-Fh sample is shown, in which O, F, Mg and Si elements are observed (note: Li element is not present since it is undetectable by this technique). The right panel of Fig. 5a shows the EDS spectrum of Na-Fh sample cation exchanged from initial Li-Fh sample. The Na element is now present although the cation exchange process took only 5 minutes. EDS spectra taken
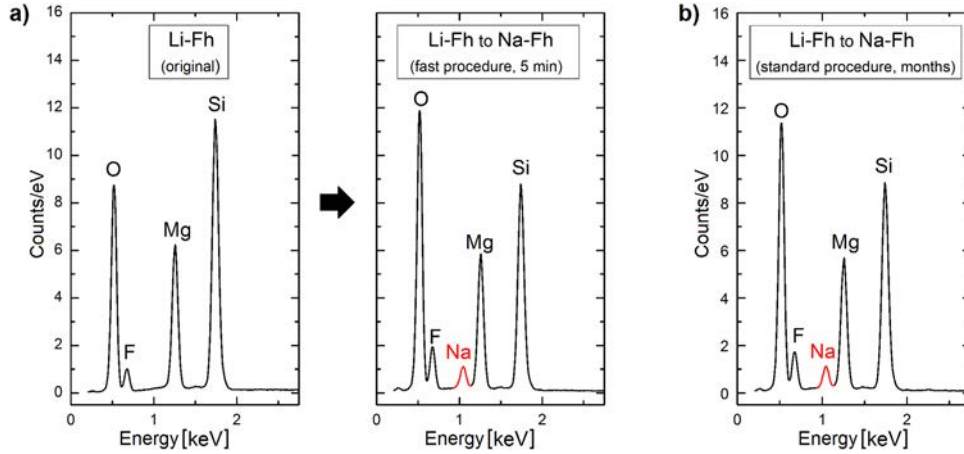
Fig. 5. a) EDS spectra of original Li-Fh sample (left panel) and Na-Fh sample after 5 minutes of cation exchange (middle panel). b) Na-Fh obtained from Li-Fh, usually performed during time-scales of months as explained in the text.

from the Na-Fh sample obtained from Li-Fh via the "traditional" procedure, and the EDS spectrum of the "original" Li-Fh are compared, see discussion below.

4 Discussions

From a diffractogram one can convert the Bragg peaks' positions to interlayer distances of the clay mineral by using Eq. (2):

$$d_{(001)} = \frac{2\pi}{q_c} \tag{2}$$

where $d_{(001)}$ is the distance between two consecutive layers of the clay mineral, as shown in Fig. 1d, and q_c is the peak position. One should also note that this information is related to the amount of water or content within the interlayer space. Whenever smectite clay minerals are in the presence of water or humid environment, they swell causing the $d_{(001)}$ to increase. The interlayer cation plays an essential role in this case, since the water molecules form different complex structures around the cations. For instance, Hemmen *et al.* found for Na-Fh, at RH = 40%, $d_{(001)} \sim 1.25$ nm. [6] and Tenório *et al.* found that the number of water molecules per Na^+ is 3.2 [23], whereas for Li-Fh the number of water molecules per Li^+ is 3 [24] and $d_{(001)} \sim 1.21$ nm. So it is possible to use $d_{(001)}$ to identify which cation is present in the interlayer space of the clay mineral.

In the present work, at RH = 27.40%, the difference between the fluorohectorites studied is the interlayer cation, which means that $d_{(001)}$ should signalize the interlayer cation within the interlayer space. Using Eq. (2) for the Bragg peaks positions of the original Li-Fh and traditional Ni-Fh (Fig. 2), the interlayer spaces are 1.206 nm and 1.453 nm respectively.

For the cation exchange of original Li-Fh to Ni-Fh after few minutes, the $d_{(001)}$ is 1.452 nm, which has the same order of magnitude of the traditionally prepared Ni-Fh (Fig. 3). This suggests that the initial cation exchange dynamics is fast and of the order of 1 minute since no trace of a (001) Li-Fh peak can be observed in neither of the pH = 2 nor pH = 7 samples.
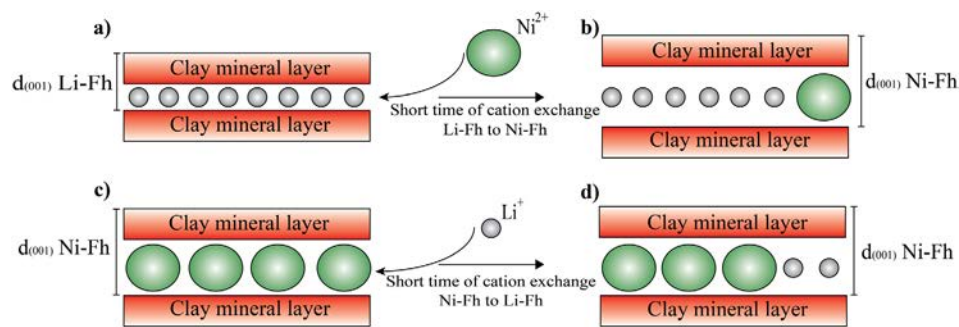
Fig. 6. Representation of a) cation exchange from original Li-Fh to Ni-Fh. b) Only few Ni^{2+} are necessary to change the interlayer space of the sample to one similar to Ni-Fh. c) Cation exchange from the traditional Ni-Fh to Li-Fh. d) The observed interlayer space after 5 minutes is similar to Ni-Fh suggesting that the $d_{(001)}$ will only decrease after most of the Ni^{2+} leave the interlayer space.

Although the $d_{(001)}$ transition from original Li-Fh is fast (few minutes), the reverse path from traditional Ni-Fh to Li-Fh is not. Since after 5 minutes of cation exchange from traditional Ni-Fh to Li-Fh the interlayer space $d_{(001)}$ is 1.451 nm (Fig. 4), which also similar to the traditionally prepared Ni-Fh. Figure 6 is a schematic representation of the cation exchange process for both directions.

The XRD data (Fig. 4) show that Ni^{2+} requires few seconds to move into the interlayer space of the fluorohectorite causing $d_{(001)}$ to increase. However, the change in the interlayer space $d_{(001)}$ from traditionally prepared Ni-Fh to Li-Fh was not observed.

As a complementary technique EDS was performed to measure the chemical composition of the sample after 5 minutes of cation exchange from Li-Fh to Na-Fh. The results show that the EDS Na peak appears after 5 minutes of cation exchange confirming the time-scale observed in XRD results.

It is expected that the cation exchange, in the present work, is only partially completed since neither XRD nor EDS can detect the signal from Li atoms. Thus one cannot exclude the possibility that some Li^+ could coexist with Ni^{2+} in the interlayers, as shown in Fig. 6. This suggests that the dynamics of the cation exchange from a larger cation, like Na^+ and Ni^{2+}, to a smaller cation, like Li^+, cannot be measured using only the techniques employed in this work.

Although the XRD and EDS are well suited technique to study the dynamics of the cation exchange from a Li^+ to either Ni^{2+} or Na^+, they are not suited to study reverse path from a either Ni^{2+} or Na^+ to the smaller Li^+. For this purpose others techniques should be used, like NMR, which was previously used to study Na-Fh and Li-Fh [24], and Inelastic Neutron Scattering, which was employed by Bordallo *et al.* to study the effects of the cations in the dynamics of the confined water in the interlayer space of a clay mineral [40].

5 Conclusions

In this work we used synchrotron XRD to investigate the cation exchange dynamic process starting from the original Li-Fh system towards a Ni-Fh or Na-Fh. The process consisted of mixing Li-Fh and salt ($NiCl_2 6(H_2O)$ to replace Li^+ with Ni^{2+} in the interlayer space and NaCl to exchange Li^+ with Na^+) in aqueous solution for two different pH values. The $d_{(001)}$ of the samples at different times show that the interlayer space is of the same order of magnitude as traditional Ni-Fh. The $d_{(001)}$ of

the samples changed in a time interval, which is shorter than one minute, and no influence of the pH could be observed. The results show that the transitions from Li^+ to a larger cation like Na^+ and Ni^{2+} is faster than 5 minutes. This was confirmed by EDS measurements. However, for the reverse path, from the traditional Ni-Fh to Li-Fh, the change in the $d_{(001)}$ was not observed during the same time scale.

Future investigations should include studies of higher order peaks in order to perform the Williamson-Hall analysis, where we will be able to obtain the strain contribution during cation exchange processes. This can provide information about the completeness of the cation exchange process due to possible buckling of the clay mineral lamella that may occur if there is a mixture of intercalated ions of different charge and size. Techniques like NMR and Inelastic Neutron Scattering should be utilized order to complete the picture of the cation exchange, since both can observe the Li^+ and the dynamics of the interlayers in a time scale of less than 1 minute [40,41].

References

1. F. Bergaya, B.K.G. Theng, G. Lagaly (eds.), *Handbook of Clay Science* (Elsevier, Amsterdam, 2006)
2. D.R. Hines, G.T. Seidler, M.M.J. Treacy, S.A. Solin, Solid State Commun. **101**, 835 (1997)
3. P. Dommersnes, Z. Rozynek, A. Mikkelsen, R. Castberg, K. Kjerstad, K. Hersvik, J. Otto Fossum, Nat. Commun. **4**, 2066 (2013)
4. S.A. Solin, J. Mol. Catal. **27**, 293 (1984)
5. J.O. Fossum, Phys. A Stat. Mech. **270**, 270 (1999)
6. H. Hemmen, L.R. Alme, J.O. Fossum, Y. Meheust, Phys. Rev. E **82**, 036315 (2010)
7. M.B. McBride, T.J. Pinnavaia, M. Mortland, Am. Miner. **60**, 66 (1975)
8. L. Tang, D.L. Sparks, Soil Sci. Soc. Am. J. **57**, 42 (1993)
9. C. Chisholm-Brause, S.D. Conradson, C.T. Buscher, P.G. Eller, D.E. Morris, Geochim. Cosmochim. Acta **58**, 3625 (1994)
10. K. Verburg, P. Baveye, M.B. McBride, Soil Sci. Soc. Am. J. **59**, 1268 (1995)
11. C. Papelis, K.F. Haynes, Colloids Surf. A **107**, 89 (1996)
12. F. Muller, G. Besson, A. Manceau, V.A. Drits, Phys. Chem. Miner. **24**, 159 (1997)
13. M.L. Schlegel, L. Charlet, A. Manceau, J. Colloid Interface Sci. **220**, 392 (1999)
14. G. Løvoll, B. Sandnes, Y. Méheust, K.J. Måløy, J.O. Fossum, G.J. da Silva, M.S.P. Mundim, R. Droppa Jr., D.M. Fonseca, Phys. B Condens. Matter **370**, 90 (2005)
15. G. da Silva, J. Fossum, E. DiMasi, K. Måløy, S. Lutnæs, Phys. Rev. E **66**, 011303 (2002)
16. R.G. Gast, in *Miner. Soil Environ.*, edited by J.B. Dixon, S.B. Weed (Soil Science Society of America, Madison, WI, 1977), p. 27
17. R.N.J. Comans, Wat. Res. **21**, 1573 (1987)
18. A.C.M. Bourg, R.H. Filby, Geochim. Cosmochim. Acta **40**, 1573 (1976)
19. R. Fujii, R.B. Corey, Soil Sci. Soc. Am. J. **50**, 306 (1986)
20. E.M. Chan, M.A. Marcus, S. Fakra, M.S. ElNaggar, R A. Mathies, A.P. Alivisatos, J. Phys. Chem. A **111**, 12210 (2007)
21. H. Hemmen, E.G. Rolseth, D.M. Fonseca, E.L. Hansen, J.O. Fossum, T.S. Plivelic, Langmuir **28**, 1678 (2012)
22. M. Ghadiri, H. Hau, W. Chrzanowski, H. Agus, R. Rohanizadeh, RSC Adv. **3**, 20193 (2013)

23. R. Tenorio, L.R. Alme, M. Engelsberg, J.O. Fossum, F. Hallwass, J. Phys. Chem. C **112**, 575 (2008)
24. R.P. Tenório, M. Engelsberg, J.O. Fossum, G.J. da Silva, Langmuir **26**, 9703 (2010)
25. A. Zegeye, S. Yahaya, C.I. Fialips, M.L. White, N.D. Gray, D.a.C. Manning, Appl. Clay Sci. **86**, 47 (2013)
26. G. da Silva, J. Fossum, E. DiMasi, K. Måløy, Phys. Rev. B **67**, 094114 (2003)
27. E.L. Hansen, H. Hemmen, D.M. Fonseca, C. Coutant, K.D. Knudsen, T.S. Plivelic, D. Bonn, J.O. Fossum, Sci. Rep. **2**, 618 (2012)
28. L. Michels, L. Ribeiro, M.S.P. Mundim, M.H. Sousa, R. Droppa Jr., J.O. Fossum, G.J. da Silva, K.C. Mundim, Appl. Clay Sci. **96**, 60 (2014)
29. N.T. Skipper, A.K. Soper, J.D.C. McConnell, K. Refson, Chem. Phys. Lett. **166**, 141 (1990)
30. G.A. Kolta, I. Novak, S.Z. El-Tawil, K.A. El-Barawy, J. Appl. Chem. Biotechnol. **26** 355 (1976)
31. E. Srasra, F. Bergaya, H. Van Damme, N.K. Ariguib, Appl. Clay Sci. **4**, 411 (1989)
32. J.-F. Lambert, G. Poncelet, Top. Catal. **4**, 43 (1997)
33. B. Cicel, P. Komadel, in *Quant. Methods Soil Mineral.*, edited by J.E. Amonette, L.W. Zelazny (Miscellaneous Publication, Madison, WI, 1994), p. 114
34. E. Wiedemann, A. Heintz, R.N. Lichtenthaler, J. Memb. Sci. **141**, 215 (1998)
35. P. Sridhar, G. Subramaniam, J. Memb. Sci. **45**, 273 (1989)
36. R. Dähn, A. Scheidegger, Geochim. Cosmochim. Acta **66**, 2335 (2002)
37. Y. Oztekin, Z. Yazicigil, Desalination **212**, 62 (2007)
38. Y. Tanaka, S.-H. Moon, V.V. Nikonenko, T. Xu, Int. J. Chem. Eng. **2012**, 1 (2012)
39. H. Strathmann, A. Grabowski, G. Eigenberger, Ind. Eng. Chem. Res. **52**, 10364 (2013)
40. H.N. Bordallo, L.P. Aldrige, G.J. Churchman, W.P. Gates, M.T. Telling, K. Kiefer, P. Fouquet, T. Seydel, S.A.J. Kimber, J. Phys. Chem. **112**, 13982 (2008)
41. W.P. Gates, H.N. Bordallo, L.P. Aldridge, T. Seydel, H. Jacobsen, V. Marry, G.J. Churchman, J. Phys. Chem. C **116**, 5558 (2012)